Extended Abstracts of the 2004 International Conference on Solid State Devices and Materials, Tokyo, 2004, pp. 98-99

F-2-4

A New Camel-Gate Field Effect Transistor with a Composite Channel Structure

Po-Hsien Lai[1], Chih-Hung Yen[1], Chung-I Kao[1], Hung-Ming Chuang[1], Sheng-Fu Tsai[1], Chun-Yuan Chen[1], and Wen-Chau Liu[1,*]

[1]Institute of Microelectronics, Department of Electrical Engineering, National Cheng-Kung University,
1 University Road, Tainan, TAIWAN 70101, Republic of China.
Phone: +886-6-209-4786 or 886-6-234-5482
*Corresponding author. E-mail: wcliu@mail.ncku.edu.tw

1. Introduction

It is known that, high electron mobility transistors (HEMTs) exhibit excellent DC and microwave performances. Also, doped-channel FETs (DCFETs) exhibit good transistor performances without the drawback of parallel conduction as found in HEMTs [1]. However, the device characteristics of DCFETs and HEMTs are affected seriously by the quality of metal-semiconductor (MS) Schottky contact. Thus, camel-gate FETs (CAMFETs) are reported to overcome this disadvantage [2]. In this work, a new HFET with an n^+-InGaP/p^+-InGaP/GaAs camel-gate and InGaAs/GaAs composite channel structure has been fabricated and demonstrated. The employed n^+-InGaP/p^+-InGaP/n-GaAs camel-gate provides a larger barrier height. In addition, composite channels, i.e., the use of n-InGaAs channel to improve the carrier transport properties and n-GaAs channel to increase the operation capability under higher electric field, are employed in the studied device. Therefore, good DC and microwave properties and higher temperature operation capability are simultaneously obtained.

2. Experimental

The epitaxial structure of the studied device was grown on a (100) oriented semi-insulating (S.I.) GaAs substrate by a metal-organic chemical vapor deposition (MOCVD) system. The schematic layers structure is illustrated in Fig. 1. The layers structure consisted of a 0.3μm GaAs buffer, a 500Å $In_{0.49}Ga_{0.51}P$ buffer, a 500Å GaAs channel (n=5 × 10^{17} cm^{-3}), a 200Å $In_{0.1}Ga_{0.9}As$ channel (n=2.5 × 10^{17} cm^{-3}), a 1000Å GaAs (n=1 × 10^{17} cm^{-3}), a 300Å $In_{0.49}Ga_{0.51}P$ (p^+=3 × 10^{18} cm^{-3}), and a 300-Å $In_{0.49}Ga_{0.51}P$ (n^+=3 × 10^{18} cm^{-3}) layer. For device fabrication, drain-source Ohmic contacts were formed on the n-GaAs layer by alloying evaporated AuGeNi/Au metals at 400 °C for 30s. The wet chemical etching process was used for device isolation. Finally, the gate contacts were achieved by evaporating AuGeNi/Au metals on n^+-InGaP cap layer with the gate dimension of 1×100 μm^2.

3. Results and Discussion

As shown in Fig. 1, the n^+-InGaP/p^+-InGaP/n-GaAs structure and n-GaAs/n-InGaAs/n-GaAs structures form the camel-like barrier gate and heterostructure channel, respectively. The corresponding conduction-band diagram is also illustrated in Fig. 1. Due to the presented conduction-band discontinuity (ΔE_C) and valance-band discontinuity (ΔE_V) at the InGaP/GaAs heterointerface, the n^+-InGaP/p^+-InGaP/n-GaAs camel-gate provides a larger barrier height which improves the carrier confinement as compared with the n^+-GaAs/p^+-GaAs/n-GaAs homo-junction camel diode [3]. In addition, the GaAs/InGaAs/GaAs composite channel layers can substantially improve carrier transport properties and device performances. The upper $In_{0.49}Ga_{0.51}P$ layer provides the higher barrier camel-gate structure and the lower $In_{0.49}Ga_{0.51}P$ layer can suppress the leakage current through the substrate leakage path. Also, the wide-gap $In_{0.49}Ga_{0.51}P$ material takes advantages of low DX centers and low reactivity with oxygen as compared to AlGaAs material.

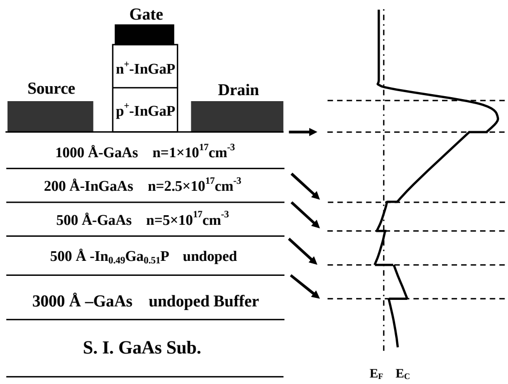

Fig. 1 The device structure and the corresponding conduction-band diagram of the studied device.

The typical gate-drain current-voltage (I-V) characteristics of the studied device at 300 to 420K are shown in Fig. 2. The forward turn-on voltage V_{on} and reverse gate leakage current I_G at V_{GD}=-10 V as a function of temperature are revealed in the upper inset of Fig. 2. The lower inset of Fig. 2 shows the temperature dependence of breakdown voltage V_{BD}. Based on the good properties of InGaP-based camel-gate, a small degradation rate in V_{on} of –0.5 mV/K is found with increasing the temperature. The gate leakage current and breakdown voltage are increased and decreased with increasing the temperature, respectively. In the studied device, the high-barrier n^+-InGaP/p^+-InGaP/n-GaAs camel diode is used to prevent

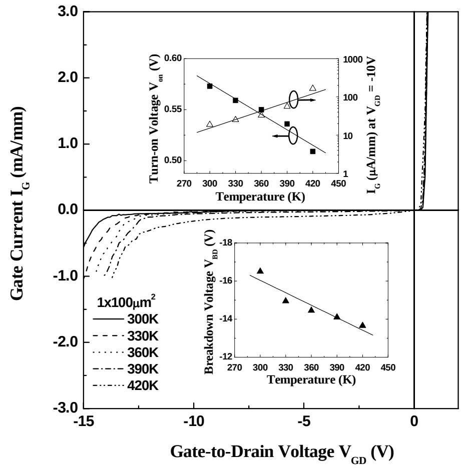

Fig. 2 The gate-drain I-V characteristics. The upper inset shows the V_{on} and I_G at V_{GD}= -10 V as a function of temperature. The lower inset shows the temperature dependence of breakdown voltage V_{BD}.

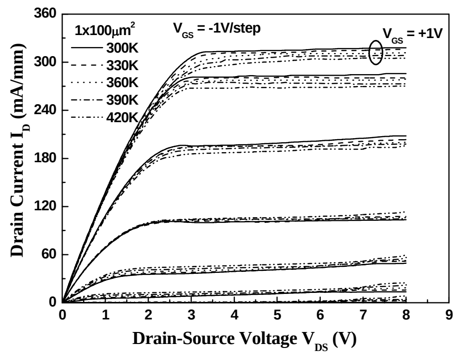

Fig. 3 The common-source output I-V characteristics of the studied device at different temperature.

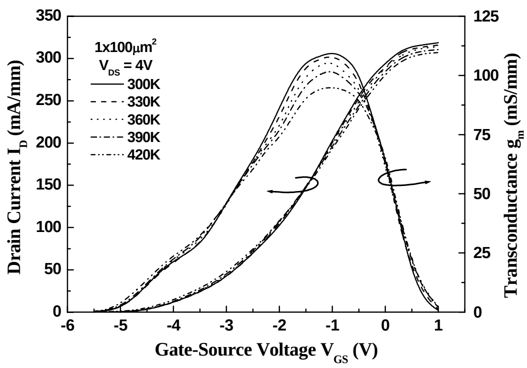

Fig. 4 The I_{DS} and g_m versus V_{GS} at different temperature.

carriers tunneling toward gate electrode. Thus, even at high temperature, the device also reveals the relatively low leakage behaviors.

The typical common-source output I-V characteristics of the studied device are shown in Fig. 3. Obviously, the degraded pinch-off and saturation characteristics associated with poor carrier confinement caused by the increase of temperature are not observed in the studied device. Figure 4 illustrates the drain saturation current I_D and transconductance g_m versus gate-source voltage V_{GS}. The maximum transconductance $g_{m,max}$ are 111.5 and 101.2 mS/mm at 300 and 420K, respectively. In addition, the maximum drain saturation current $I_{D,max}$ of 318.7 and 307.0 mA/mm are found at 300 and 420K, respectively. The $I_{D,max}$ value at 420K still maintains 96% of its value at 300K. This is certainly suitable for high-temperature applications.

The microwave performances of the studied device are shown in Fig. 5. The unity current gain cut-off frequency f_T and maximum oscillation frequency f_{max} values of 16.2 and 24.2 GHz are observed. The inset of Fig. 5 shows the f_T and f_{max} versus gate-source voltage. Clearly, a wide gate voltage operation regime over 3V with good microwave performances is obtained.

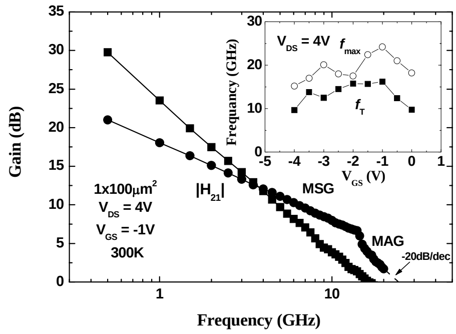

Fig. 5 The device structure and the corresponding conduction-band diagram of the studied device.

4. Conclusion

In summary, an interesting CAMFET with the n^+-InGaP/p^+-InGaAs/GaAs camel-gate and GaAs/InGaAs composite channel structure is fabricated and demonstrated. The temperature dependent characteristics are also studied. Experimentally, this studied device shows good DC and RF characteristics including lower leakage current, higher breakdown voltage, transconductance, voltage gain, f_T, and f_{max}, etc.. Furthermore, the relatively negligibly temperature-dependent performances over wide temperature range of 300K<T<420K are observed. Consequentially, the studied device provides the promise for high-temperature and high-performance microwave electronic applications.

Acknowledgements

Part of this work was supported by the National Science Council of the Republic of China under Contract No. NSC-92-2215-E-006-007. The authors are also grateful to National Nano Device Laboratories (NDL) for RF measurements.

References

[1] W. C. Hsu, H. M. Shieh, C. L. Wu, and T. S.Wu IEEE Trans. Electron Devices **41** (1994) 456.

[2] M. Marso, G. Zwinge, D. Grutzmacher, J. Hergeth, and H. Beneking IEE Electron. Lett. **27** (1991) 335.

[3] W. S. Lour, J. H. Tsai, L. W. Laih, and W. C. Liu IEEE Trans. Electron Devices **43** (1996) 871.